

PHYSARUM DYNAMICS AND OPTIMAL TRANSPORT FOR BASIS PURSUIT

ENRICO FACCA, FRANCO CARDIN AND MARIO PUTTI

ABSTRACT. We study the connections between Physarum Dynamics and Dynamic Monge Kantorovich (DMK) Optimal Transport algorithms for the solution of Basis Pursuit problems. We show the equivalence between these two models and unveil their dynamic character by showing existence and uniqueness of the solution for all times and constructing a Lyapunov functional with negative Lie-derivative that drives the large-time convergence. We propose a discretization of the equation by means of a combination of implicit time-stepping and Newton method yielding an efficient and robust method for the solution of general basis pursuit problems. Finally, we propose a simple modification to the dynamic equation that can be interpreted as a gradient flow system for the Lyapunov functional. Several numerical experiments run on literature benchmark problems are used to show the accuracy, efficiency, and robustness of the proposed method.

1. INTRODUCTION

In recent years, a slime mold called *Physarum Polycephalum* (PP) captured the interest of many authors for its optimization abilities first described in [14, 17]. The first attempt to encode the optimization behavior of PP into a mathematical modeling framework was proposed in [16]. Here, the slime mold body is schematized as a graph $G = (V, E)$ with n vertices $v \in V$ and m edges $e \in E$ of length $w_e > 0$. Given a time interval $I = [0, \infty)$, denoting with A the adjacency matrix of G , with $\mathbf{w} = \{w_e\}$ the vector of edge lengths, and with $\mathbf{f} : V \mapsto \mathbb{R}$ a vector of forcing values such that $\sum_{v \in V} f_v = 0$, the Physarum Dynamics (PD) proposed by [16] tries to find the curves $\boldsymbol{\mu}(t) : I \mapsto \mathbb{R}^m$ and $\mathbf{u}(t) : I \mapsto \mathbb{R}^n$ that solve the following equations:

$$(1a) \quad \mathbf{q}(t) = C[\boldsymbol{\mu}(t)] W^{-1} A^T \mathbf{u}(t); \quad C[\boldsymbol{\mu}(t)] = \text{diag}(\boldsymbol{\mu}(t)); \quad W = \text{diag}(\mathbf{w}) ,$$

$$(1b) \quad A\mathbf{q}(t) = \mathbf{f} ,$$

$$(1c) \quad \partial_t \boldsymbol{\mu}(t) = |\mathbf{q}(t)| - \boldsymbol{\mu}(t) ,$$

$$(1d) \quad \boldsymbol{\mu}(0) = \hat{\boldsymbol{\mu}} > 0 ,$$

where the absolute value $|\cdot|$ is taken component-wise. In [3] it was proved that the flux $\mathbf{q}(t)$ converges as $t \rightarrow \infty$ toward a steady state equilibrium \mathbf{q}^* that solves the following weighted l_1 minimization problem on the graph G , also called *Optimal Transshipment Problem*:

$$(2) \quad \min_{\mathbf{q} \in \mathbb{R}^m} \|\mathbf{q}\|_{1,W} := \sum_{e \in E} |q_e| w_e \quad \text{s.t.}: A\mathbf{q} = \mathbf{f} ,$$

More recently, [15] extended the application of the model given by Equation (1) to general matrices $A \in \mathbb{R}^{n,m}$, arriving at a l_1 -minimization problem with weight \mathbf{w} (often equal to one) related to *Basis Pursuit* (BP). Moreover, the same authors unraveled the relationship of their approach with the Iteratively Reweighted Least Square method (IRLS), an Alternating Minimization algorithm [1] for the solution of l_1 -minimizations.

The above PD model inspired also the study in [9], where an extension to the continuous framework, called the *Dynamic Monge-Kantorovich* problem (DMK), was presented and studied. In this latter study, the authors propose a conjecture stating that the long time solution of DMK is solution to the Optimal Transport Problem (OTP) [18], and in particular the Monge-Kantorovich equations, with cost equal to the Euclidean distance, (the so-called L^1 -OTP).

The first goal of our work is to show the analogies between the L^1 -OTP and the BP problems, and between the continuum DMK model and the discrete PD model proposed by [15], extending and re-interpreting some of their results to highlight the dynamic nature of the model. We provide a novel and extended proof of uniqueness and global existence of the solution to the system of equations, and show the existence of a Lyapunov functional \mathcal{L} , i.e. a functional decreasing along solution trajectories. In addition, we re-adapt to the discrete case the proof given in [10] showing that the minimization of \mathcal{L} is equivalent to the l_1 minimization problem Equation (2).

Our second goal is to fully exploit the dynamic nature of PD from a computational point of view and use an implicit (Backward Euler) time stepping scheme combined with Newton-Raphson method to drastically reduce the computational cost of the solution of BP via PD. Finally, we show how simple modifications to our dynamics transform the PD into a *Gradient Flow* for the Lyapunov functional \mathcal{L} , and our proposed solution algorithm can be reinterpreted as an efficient steepest descent algorithm.

The paper is organized as follows. In Section 2 we describe the DMK model in the continuous setting, recalling the main results and conjectures. Section 3 starts from the semi-discrete (discretized in space) DMK problem to derive the BP dynamics and show global existence and uniqueness of the solution of the resulting ODE system. Moreover, we prove that there exist a Lyapunov functional and that its unique minimum (at infinite times) is the solution of an OTP. In this section we try to use notations that are similar to the continuous case to highlight the similarities between the two problems, and use the duality relationships between the gradient and divergence operators. The next section develops our final algorithm, introducing the implicit time discretization (backward Euler) and Newton method. In addition, the extension leading to the gradient flow structure is presented. Finally, a set of numerical results are used to show the efficiency and robustness of our algorithm.

2. FROM PHYSARUM DYNAMICS TO DYNAMIC MONGE-KANTOROVICH

We start this section by recalling the main results proposed in [9, 10] in the continuous setting. The DMK model can be described as follows. Consider a convex, bounded and smooth domain $\Omega \in \mathbb{R}^d$, a function $f \in L^2(\Omega)$ with $\int_{\Omega} f = 0$, and a strictly positive function μ_0 on Ω . We want to find the pair of functions $u : I \times \Omega \mapsto \mathbb{R}$ and $\mu : I \times \Omega \mapsto \mathbb{R}$ solving:

$$(3a) \quad -\operatorname{div}(\mu \nabla u) = f ,$$

$$(3b) \quad \partial_t \mu = |\mu \nabla u| - \mu ,$$

$$(3c) \quad \mu(0, x) = \mu_0(x) ,$$

where the first equation is intended in a weak sense and is completed with zero Neumann Boundary conditions. In [9] it was conjectured that the solution of the above problem converges as $t \rightarrow \infty$ to a steady state configuration (μ^*, u^*) solution of the so-called Monge-Kantorovich Equation, a PDE based formulation of the L^1 -OTP [8].

Denoting with $U[\bar{\mu}]$ the weak solution of $-\operatorname{div}(\bar{\mu}\nabla\bar{u}) = f$ for a given $\bar{\mu} > 0$, system Equation (3) is converted into the following ordinary differential equation in Banach space:

$$(4a) \quad \partial_t \mu = \mu |\nabla U[\mu]| - \mu ,$$

$$(4b) \quad \mu(0) = \mu_0 .$$

The existence of a global solution of Equation (4) is still an open question and so is convergence toward equilibrium. However, in [9, 10] the following results are proved:

Proposition 1. *There exists a $\bar{t} > 0$ such that Equation (4) has a unique solution $\mu(t)$ for all $t \in [0, \bar{t}[$ that bounded from below by $e^{-t} \min(\mu_0)$. Moreover the functional*

$$(5) \quad \mathcal{L}(\mu) := \mathcal{E}(\mu) + \mathcal{M}(\mu) ,$$

$$\mathcal{E}(\mu) := \sup_{\varphi \in Lip(\Omega)} \int_{\Omega} \left(f\varphi - \mu \frac{|\nabla\varphi|^2}{2} \right) dx \quad \mathcal{M}(\mu) := \frac{1}{2} \int_{\Omega} \mu dx ,$$

is a Lyapunov functional for Equation (4), with derivative along the $\mu(t)$ -trajectory given by:

$$(6) \quad \frac{d}{dt} (\mathcal{L}(\mu(t))) = -\frac{1}{2} \int_{\Omega} \mu(t) (|\nabla U[\mu(t)]| + 1) (|\nabla U[\mu(t)]| - 1)^2 dx .$$

In addition, $\mathcal{L}(\mu)$ admits a unique minimizer μ^* , the so-called OT density, and the following equalities hold:

$$(7) \quad \min_{\mu \in L^1(\Omega)} \mathcal{L}(\mu) = \min_{v \in [L^1(\Omega)]^d} \left\{ \int_{\Omega} |v| dx : -\operatorname{div}(v) = f \right\} = \max_{u \in Lip_1(\Omega)} \left\{ \int_{\Omega} u f dx \right\} ,$$

where the unique minimizers μ^* and v^* , and the non-unique maximizer u^* are related by the following equation:

$$(8) \quad v^* = \mu^* \nabla u^* .$$

Remark 1. *For a strictly positive measure μ the energy functional $\mathcal{E}(\mu)$ can be written equivalently as:*

$$(9) \quad \mathcal{E}(\mu) = \frac{1}{2} \int_{\Omega} \mu |\nabla U[\mu]|^2 dx .$$

3. FROM DYNAMIC MONGE-KANTOROVICH TO BASIS PURSUIT

The semi-discrete version of Equation (3) obtained after spatial discretization by e.g. the finite element method as done in [10] is related to Equation (1). Indeed, assuming for simplicity that matrix A in Equation (2) is of full-rank, using the matrices W and $C[\boldsymbol{\mu}]$ defined in Equation (1a) and the additional matrices:

$$(10) \quad \nabla := W^{-1}A^T \quad S[\boldsymbol{\mu}] := AC[\boldsymbol{\mu}]W^{-1}A^T ,$$

we can rewrite Equation (1) as follows:

$$(11a) \quad S[\boldsymbol{\mu}(t)]\mathbf{u}(t) = \mathbf{f} ,$$

$$(11b) \quad \partial_t \boldsymbol{\mu}(t) = |\mathbf{q}(t)| - \boldsymbol{\mu}(t)$$

$$= |C[\boldsymbol{\mu}(t)]W^{-1}A^T\mathbf{u}(t)| - \boldsymbol{\mu}(t) = |C[\boldsymbol{\mu}(t)]\nabla\mathbf{u}(t)| - \boldsymbol{\mu}(t)$$

$$(11c) \quad \boldsymbol{\mu}(0) = \hat{\boldsymbol{\mu}} > 0 ,$$

where as before the absolute value of a vector $|\cdot|$ is intended element-by-element. We can identify in $S[\boldsymbol{\mu}(t)]$ the finite element stiffness matrix for a given $\boldsymbol{\mu}$ and

in $\nabla \mathbf{u}(t) = W^{-1} A^T \mathbf{u}(t)$ the discretization of the gradient of $U[\boldsymbol{\mu}(t)]$. This semi-discrete algorithm is the same as the one proposed in [15] for the solution of the Basis Pursuit problem. Analogously to the continuous case, given a strictly positive $\boldsymbol{\mu}$, we define $\mathbf{U}[\boldsymbol{\mu}]$ as the solution of the linear system $S[\boldsymbol{\mu}] \mathbf{u} = \mathbf{f}$ and rewrite Equation (11) in the following system of ODEs:

$$(12a) \quad \partial_t \boldsymbol{\mu}(t) = C[\boldsymbol{\mu}(t)] |\nabla \mathbf{U}[\boldsymbol{\mu}(t)]| - \boldsymbol{\mu}(t),$$

$$(12b) \quad \boldsymbol{\mu}(0) = \hat{\boldsymbol{\mu}} > 0.$$

Now we are able to prove that the solution of the above problem exists and is unique for all times and that this dynamics admits a unique long-time equilibrium solution. Moreover we can define a Lyapunov functional whose minimizer is solution of a discrete optimal transport problem. Indeed, we have the following results:

Proposition 2. *Equation (12) has a global unique solution for all $t \in I$ and admits a Lyapunov functional given by:*

$$(13) \quad \mathcal{L}(\boldsymbol{\mu}) := \mathcal{E}(\boldsymbol{\mu}) + \mathcal{M}(\boldsymbol{\mu}),$$

$$(14) \quad \mathcal{E}(\boldsymbol{\mu}) = \sup_{\mathbf{u} \in \mathbb{R}^n} \left\{ \mathbf{f}^T \mathbf{u} - \frac{1}{2} \mathbf{u}^T S[\boldsymbol{\mu}] \mathbf{u} \right\} \quad \mathcal{M}(\boldsymbol{\mu}) := \frac{1}{2} \boldsymbol{\mu}^T \mathbf{w}.$$

The derivative of \mathcal{L} along the $\boldsymbol{\mu}(t)$ -trajectory takes on the form:

$$(15) \quad \frac{d}{dt} \mathcal{L}(\boldsymbol{\mu}(t)) = -\frac{1}{2} \sum_{e=1}^m \mu_e(t) (|\nabla \mathbf{u}(t)|_e + 1) (|\nabla \mathbf{u}(t)|_e - 1)^2 w_e.$$

and the following equalities hold:

$$(16) \quad \min_{\boldsymbol{\mu} \in \mathbb{R}_{\geq 0}^m} \mathcal{L}(\boldsymbol{\mu}) = \min_{\mathbf{q} \in \mathbb{R}^m} \left\{ \|\mathbf{q}_e\|_{1,W} : A\mathbf{q} = \mathbf{f} \right\} = \max_{\mathbf{u} \in \mathbb{R}^n} \left\{ \mathbf{u}^T \mathbf{f} : \|\nabla \mathbf{u}\|_{l_\infty} \leq 1, \right\}$$

where the unique minimizers $\boldsymbol{\mu}^*$ and \mathbf{q}^* , and the non-unique maximizer \mathbf{u}^* are related by the following equation:

$$(17) \quad \mathbf{q}^* = \text{diag}(\boldsymbol{\mu}^*) \nabla \mathbf{u}^* = C[\boldsymbol{\mu}^*] \nabla \mathbf{u}^*.$$

Remark 2. *As in the continuous case, for strictly positive $\boldsymbol{\mu}$ the energy functional $\mathcal{E}(\boldsymbol{\mu})$ can be written in analogy to the continuous case in the following alternative forms:*

$$(18) \quad \mathcal{E}(\boldsymbol{\mu}) = \frac{1}{2} (\nabla \mathbf{U}[\boldsymbol{\mu}])^T W C[\boldsymbol{\mu}] \nabla \mathbf{U}[\boldsymbol{\mu}] = \frac{1}{2} (\mathbf{U}[\boldsymbol{\mu}])^T S[\boldsymbol{\mu}] \mathbf{U}[\boldsymbol{\mu}].$$

The proof of the previous proposition requires the following lemma whose proof can be found in [7] (see also [4] for the continuous analogue).

Lemma 1. *Given $\boldsymbol{\mu} \in \mathbb{R}_+^m$, non-negative, and $\mathbf{f} \in \text{Im}(A)$, the following equalities hold:*

$$(19) \quad \mathcal{E}(\boldsymbol{\mu}) = \sup_{\mathbf{u} \in \mathbb{R}^n} \left\{ \mathbf{f}^T \mathbf{u} - \frac{1}{2} \mathbf{u}^T S[\boldsymbol{\mu}] \mathbf{u} \right\} = \inf_{\boldsymbol{\xi} \in \mathbb{R}_{\boldsymbol{\mu}, \mathbf{w}}^n} \left\{ \frac{1}{2} \langle \boldsymbol{\xi}, \boldsymbol{\xi} \rangle_{\boldsymbol{\mu}, W} : A C[\boldsymbol{\mu}] \boldsymbol{\xi} = \mathbf{f} \right\},$$

where $\mathbb{R}_{\boldsymbol{\mu}, \mathbf{w}}^n$ denote \mathbb{R}^n with scalar product $\langle \mathbf{x}, \mathbf{y} \rangle_{\boldsymbol{\mu}, W} := (C[\boldsymbol{\mu}] W \mathbf{x})^T \mathbf{y}$.

Proof of Proposition 2. We first prove local existence and uniqueness of the solution $\boldsymbol{\mu}(t)$ of Equation (12). For any initial data $\hat{\boldsymbol{\mu}} > 0$, there exists a neighborhood $B_{\hat{\boldsymbol{\mu}}}$ where all $\boldsymbol{\mu} \in B_{\hat{\boldsymbol{\mu}}}$ are strictly positive. Let $\mathbf{U}[\cdot] : B_{\hat{\boldsymbol{\mu}}} \mapsto \mathbb{R}^n$ be the operator defined by $\mathbf{U}[\boldsymbol{\mu}] = (S[\boldsymbol{\mu}])^{-1} \mathbf{f}$. By the Cayley-Hamilton theorem, the vector $(S[\boldsymbol{\mu}])^{-1} \mathbf{f}$ is a combination of sums, products, and reciprocals of the elements of $\boldsymbol{\mu}$ and hence is infinitely differentiable (\mathcal{C}^∞). Now, all terms on the right-hand side of Equation (12) are Lipschitz-continuous and we can invoke Banach-Caccioppoli

fixed point theory to guarantee existence and uniqueness of a solution $\boldsymbol{\mu}(t)$ for $t \in [0, \bar{t}]$, with \bar{t} depending on $\hat{\boldsymbol{\mu}}$ and \mathbf{f} . From the mild solution of Equation (12) the lower bound $\boldsymbol{\mu}(t) \geq e^{-t} \min(\hat{\boldsymbol{\mu}})$ is easily derived, showing that $\boldsymbol{\mu}$ is strictly positive for $\hat{\boldsymbol{\mu}} > 0$. This observation directly yields global existence and uniqueness of $\mathbf{U}[\boldsymbol{\mu}(t)]$ for all $t > 0$.

To prove Equation (15), take the solution pair $(\mathbf{u}(t), \boldsymbol{\mu}(t))$ of Equation (11) for $t \in [0, \bar{t}]$, where $\mathbf{u}(t) = \mathbf{U}[\boldsymbol{\mu}(t)]$. We want to compute the time derivative of $\mathcal{E}(\boldsymbol{\mu}(t))$:

$$(20) \quad \begin{aligned} \frac{d}{dt} \mathcal{E}(\boldsymbol{\mu}(t)) &= \frac{1}{2} \frac{d}{dt} (\mathbf{u}^T(t) S[\boldsymbol{\mu}(t)] \mathbf{u}(t)) , \\ &= \frac{1}{2} (2\mathbf{u}^T(t) S[\boldsymbol{\mu}(t)] \partial_t \mathbf{u}(t) + \mathbf{u}^T(t) S[\partial_t \boldsymbol{\mu}(t)] \mathbf{u}(t)) . \end{aligned}$$

Differentiating with respect to time the system $S[\boldsymbol{\mu}(t)] \mathbf{u}(t) = \mathbf{f}$ we obtain:

$$S[\partial_t \boldsymbol{\mu}(t)] \mathbf{u}(t) + S[\boldsymbol{\mu}(t)] \partial_t \mathbf{u}(t) = 0 .$$

Multiplication of both sides by $\mathbf{u}^T(t)$ yields:

$$\mathbf{u}^T(t) S[\boldsymbol{\mu}(t)] \partial_t \mathbf{u}(t) = -\mathbf{u}^T(t) S[\partial_t \boldsymbol{\mu}(t)] \mathbf{u}(t) .$$

Substituting the last equation in Equation (20), we can express the time derivative of the energy as:

$$\frac{d}{dt} \mathcal{E}(\boldsymbol{\mu}(t)) = -\frac{1}{2} \mathbf{u}^T(t) S[\partial_t \boldsymbol{\mu}(t)] \mathbf{u}(t) = -\frac{1}{2} (\nabla \mathbf{u}(t))^T W C[\partial_t \boldsymbol{\mu}(t)] \nabla \mathbf{u}(t) .$$

Adding the time derivative of the mass functional $\mathcal{M}(\boldsymbol{\mu}(t))$, a few simple algebraic manipulations yield Equation (15).

Global existence and uniqueness of the solution vector $\boldsymbol{\mu}(t)$ at all times $t \in I$ now follows. Indeed, the time derivative of $\mathcal{L}(\boldsymbol{\mu}(t))$ is strictly negative and thus $\boldsymbol{\mu}(t)$ is forced to live for all times $t > 0$ in a weighted l_1 -ball of \mathbb{R}^m with radius $\mathcal{L}(\boldsymbol{\mu}(0))$, as the following inequality states:

$$\|\boldsymbol{\mu}(t)\|_{1,W} = \mathcal{M}(\boldsymbol{\mu}(t)) \leq \mathcal{E}(\boldsymbol{\mu}(t)) + \mathcal{M}(\boldsymbol{\mu}(t)) = \mathcal{L}(\boldsymbol{\mu}(t)) \leq \mathcal{L}(\boldsymbol{\mu}(0)) .$$

From this, we automatically obtain global existence for Equation (12) by applying well know results on maximal solutions of ODEs [12, Corollary 3.2].

To prove Equation (16) we use the results of the duality Lemma 1 to rewrite the energy functional $\mathcal{E}(\boldsymbol{\mu})$ in the following variational form:

$$\mathcal{E}(\boldsymbol{\mu}) = \inf_{\boldsymbol{\xi} \in \mathbb{R}_{\boldsymbol{\mu}}^m} \left\{ \frac{1}{2} \sum_{e \in E} \xi_e^2 \mu_e w_e : AC[\boldsymbol{\mu}] \boldsymbol{\xi} = \mathbf{f} \right\} .$$

Then, the Lyapunov functional \mathcal{L} can be rewritten as:

$$\mathcal{L}(\boldsymbol{\mu}) = \inf_{\boldsymbol{\xi} \in \mathbb{R}_{\boldsymbol{\mu}}^m} \frac{1}{2} \sum_{e \in E} \xi_e^2 \mu_e w_e + \frac{1}{2} \sum_{e \in E} \mu_e w_e .$$

For any $\boldsymbol{\xi} \in \mathbb{R}_{\boldsymbol{\mu}}^m, \boldsymbol{\mu} \in \mathbb{R}_+^m$, by Young inequality we obtain:

$$\sum_{e \in E} |\xi_e \mu_e| w_e = \sum_{e \in E} \left| \xi_e \mu_e^{1/2} \mu_e^{1/2} \right| \leq \frac{1}{2} \sum_{e \in E} \xi_e^2 \mu_e w_e + \frac{1}{2} \sum_{e \in E} \mu_e w_e .$$

Since the above inequality holds for any $\boldsymbol{\mu} \in \mathbb{R}_+^m$, taking the infimum over the $\boldsymbol{\xi} \in \mathbb{R}_\mu^m$ yields:

$$\begin{aligned} & \inf_{\boldsymbol{\xi} \in \mathbb{R}_\mu^m} \left\{ \sum_{e \in E} |\xi_e \mu_e| w_e : AC[\boldsymbol{\mu}] \boldsymbol{\xi} = \mathbf{f} \right\} \\ & \leq \inf_{\boldsymbol{\xi} \in \mathbb{R}_\mu^m} \left\{ \frac{1}{2} \sum_{e \in E} \xi_e^2 \mu_e w_e + \frac{1}{2} \sum_{e \in E} \mu_e w_e : AC[\boldsymbol{\mu}] \boldsymbol{\xi} = \mathbf{f} \right\} \\ & = \mathcal{L}(\boldsymbol{\mu}) \quad \forall \boldsymbol{\mu} \in \mathbb{R}_+^m, \end{aligned}$$

and thus, since $q_e = \xi_e \mu_e$, we can write:

$$\inf_{\mathbf{q} \in \mathbb{R}^m} \left\{ \sum_{e \in E} |q_e| w_e : A\mathbf{q} = \mathbf{f} \right\} \leq \inf_{\boldsymbol{\mu} \in \mathbb{R}_+^m} \mathcal{L}(\boldsymbol{\mu}).$$

Now, we let \mathbf{q}^* , \mathbf{u}^* be solutions of the problems in Equations (16) and (17) (\mathbf{u}^* is in general not unique) and consider the vector defined as:

$$\boldsymbol{\mu}^* := |q_e^*|.$$

We can write the following chain of equalities and inequalities:

$$\sum_{e \in E} |q_e^*| w_e = \inf_{\mathbf{q} \in \mathbb{R}^m} \left\{ \sum_{e \in E} |q_e| w_e : A\mathbf{q} = \mathbf{f} \right\} \leq \inf_{\boldsymbol{\mu} \in \mathbb{R}_+^m} \mathcal{L}(\boldsymbol{\mu}) \leq \mathcal{L}_1(\boldsymbol{\mu}^*) = \sum_{e \in E} |q_e^*| w_e,$$

showing that $\boldsymbol{\mu}^*$ is a minimum of the Lyapunov functional \mathcal{L} and that $q_e = \mu_e^* \nabla u_e[\boldsymbol{\mu}]$ solves Equation (2). \square

Remark 3. *We want to emphasize that, in the continuous case, the identification of the metric space where μ belongs to is a crucial step to establish the existence of solutions for the DMK model. In fact, in the infinite dimensional case, given a strictly positive measure μ_0 there exists a measure μ belonging to an arbitrarily small ball of μ_0 that is not bounded away from zero (consider, e.g., the space $L^1(\Omega)$ with the standard metric). However, in the finite dimensional setting of interest for our current work this difficulty is completely avoided.*

4. NUMERICAL DISCRETIZATION

In [15] the PD in Equation (12) is discretized with forward Euler time stepping with fix time-step. In this case, the authors show that the scheme can be interpreted as an IRLS scheme. Standard stability limitations characteristic of the forward Euler method prevent the use of large time-steps. In addition, the use of a constant time-step size does not exploit the expected exponential convergence towards steady state of the dynamical system. To overcome these difficulties, we generate the numerical approximation (minimization) sequence $(\boldsymbol{\mu}^k)$ by discretizing the dynamics (11) via the unconditionally stable backward Euler discretization with variable step size. The non-linear system resulting at each time step is solved by means of an Inexact Newton-Krylov method. The latter approach allows also the potential exploitation of the sparsity structures of matrices A , $C[\boldsymbol{\mu}]$, and W , increasing computational efficiency, as seen in the numerical examples. We describe next our implementation, show some numerical results on literature benchmarks, discussing some heuristic explanations of the behavior of the proposed scheme.

4.1. Backward Euler and Newton method. Discretization of Equation (11) by the implicit backward Euler scheme leads to the following sequence of nonlinear-algebraic equations for $(\mathbf{u}^{k+1}, \boldsymbol{\mu}^{k+1})$:

$$(21) \quad \begin{aligned} S[\boldsymbol{\mu}^{k+1}] \mathbf{u}^{k+1} &= \mathbf{f} \\ \boldsymbol{\mu}^{k+1} &= \boldsymbol{\mu}^k + \Delta t_k (C[\boldsymbol{\mu}^{k+1}] |\nabla \mathbf{u}^{k+1}| - \boldsymbol{\mu}^{k+1}) . \end{aligned}$$

We restate the nonlinear system to be solved at each time step k as the problem of finding the zero $\mathbf{z} = (\mathbf{u}, \boldsymbol{\mu})$ of the function:

$$(22) \quad \mathbf{F}(\mathbf{u}, \boldsymbol{\mu}) = \begin{pmatrix} \mathbf{F}_1(\mathbf{u}, \boldsymbol{\mu}) \\ \mathbf{F}_2(\mathbf{u}, \boldsymbol{\mu}) \end{pmatrix} = \begin{pmatrix} S[\boldsymbol{\mu}] \mathbf{u} - \mathbf{f} \\ \boldsymbol{\mu} - \Delta t_k (C[\boldsymbol{\mu}] |\nabla \mathbf{u}| - \boldsymbol{\mu}) - \boldsymbol{\mu}^k \end{pmatrix} = 0 .$$

Denoting with m the nonlinear iteration index, Newton method for finding the zero of the above function can be written as:

$$(23) \quad \begin{aligned} J(\mathbf{z}^m) \mathbf{s} &= -\mathbf{F}(\mathbf{z}^m) \\ \mathbf{z}^{m+1} &= \mathbf{z}^m + \mathbf{s} . \end{aligned}$$

The Jacobian matrix is given by:

$$(24) \quad \begin{aligned} J(\mathbf{u}, \boldsymbol{\mu}) &= \begin{pmatrix} \partial_{\mathbf{u}} \mathbf{F}_1(\mathbf{u}, \boldsymbol{\mu}) & \partial_{\boldsymbol{\mu}} \mathbf{F}_1(\mathbf{u}, \boldsymbol{\mu}) \\ \partial_{\mathbf{u}} \mathbf{F}_2(\mathbf{u}, \boldsymbol{\mu}) & \partial_{\boldsymbol{\mu}} \mathbf{F}_2(\mathbf{u}, \boldsymbol{\mu}) \end{pmatrix} , \\ &= \begin{pmatrix} S[\boldsymbol{\mu}] & AG[\mathbf{u}] \\ -\Delta t_k C[\boldsymbol{\mu}] D_1[\mathbf{u}] \nabla & D_2[\mathbf{u}] \end{pmatrix} , \end{aligned}$$

where G , D_1 , and D_2 are diagonal matrices given by:

$$G[\mathbf{u}] = \text{diag}(\nabla \mathbf{u}) \quad D_1[\mathbf{u}] = \text{diag}(\text{sign}(\nabla \mathbf{u})) \quad D_2[\mathbf{u}] = \text{diag}(\mathbf{1} - \Delta t_k (|\nabla \mathbf{u}| - \mathbf{1})) .$$

Here, the sign function is again intended element-by-element and $\mathbf{1}$ indicates the vector with all elements equal to one. Assuming that all the matrices are evaluated at \mathbf{z}^m , the Newton linear system can be reduced to the $n \times n$ symmetric system given by:

$$(25a) \quad M \mathbf{s}_1 := (S + \Delta t_k A G D_2^{-1} C D_1 \nabla) \mathbf{s}_1 = A G D_2^{-1} \mathbf{F}_2 - \mathbf{F}_1$$

$$(25b) \quad \mathbf{s}_2 = D_2^{-1} (\Delta t_k D_2^{-1} C D_1 \nabla \mathbf{s}_1 - \mathbf{F}_2) .$$

Since $\boldsymbol{\mu}$ and \mathbf{u} appear linearly, the symmetric matrix M can be rewritten as $M = S[\tilde{\boldsymbol{\mu}}]$ with $\tilde{\boldsymbol{\mu}} = \{\tilde{\mu}_e\}$ defined as:

$$\tilde{\mu}_e = \mu_e + \Delta t_k \frac{\mu_e |\nabla \mathbf{u}|_e}{1 - \Delta t_k (|\nabla \mathbf{u}|_e - 1)} = \mu_e \frac{1 + \Delta t_k}{1 - \Delta t_k (|\nabla \mathbf{u}|_e - 1)} ,$$

Note that, if Δt_k small enough, D_2 is strictly positive and thus always invertible, and matrix M is symmetric and positive definite. As supported also by the numerical evidence, in practice this requirement is always met since at large times $|\nabla \mathbf{u}|_e \approx \mathbf{1}$ and we start from $\boldsymbol{\mu}_0 > 0$. Thus the time-step size can be progressively increased as time advances.

Linear solver. We implemented an Inexact Newton method with a Preconditioned Conjugate Gradient (PCG) solver for the linear system (25a) and standard variable forcings as suggested in [6]. The matrix vector product $M \mathbf{v}$ is performed sequentially from right to left. Matrix M is formed explicitly only when calculating the preconditioner, thus allowing potential exploitation of sparsity in matrix A .

In our preliminary implementation, preconditioning is obtained by calculating the Cholesky decomposition of M and reusing it until degradation of the PCG performance is detected (number of PCG iterations larger than a specified threshold). The exit criterion is based on the preconditioned residual [13]. Note that, as time progresses, some values of μ_e tend to zero, drastically increasing the ill-conditioning

of the linear system. To cope with this problem, we use the spectral preconditioner developed in [2], which makes efficient use of partial eigenspectrum information. Time stepping strategy. At each time step, we start the Newton iteration with the converged values at the previous time step $\mathbf{z}^0 = (\mathbf{u}^k, \boldsymbol{\mu}^k)$. At every time step the value of Δt_k is doubled and a check on the positivity of the entries in D_2 is performed. If this check fails, Δt_k is decreased by a factor 2. The initial Δt_0 is typically unitary. We consider that equilibrium (or time-convergence) is achieved when:

$$(26) \quad \text{var}(\boldsymbol{\mu} [t^k]) = \frac{\|\boldsymbol{\mu}^{k+1} - \boldsymbol{\mu}^*\|}{\Delta t_{k+1} \|\boldsymbol{\mu}^*\|} < \tau_T .$$

In our numerical experiments we set $\tau_T = 5 \times 10^{-8}$.

4.2. From Physarum Dynamics to Gradient Flow for Basis Pursuit. In this paragraph we propose a simple modifications of our discrete DMK leading to a gradient flow problem for the corresponding Lyapunov functional. To this aim, starting from Equation (12), we replace the term $|\nabla \mathbf{U} [\boldsymbol{\mu}(t)]|$ with $|\nabla \mathbf{U} [\boldsymbol{\mu}(t)]|^2$, where as for the absolute value also the square power is applied element-by-element, and introduce the change of variable $\boldsymbol{\mu} = \Psi(\boldsymbol{\sigma}) = \boldsymbol{\sigma}^2/2$. We have the following Proposition:

Proposition 3. *Let $\boldsymbol{\mu} = \Psi(\boldsymbol{\sigma}) = \boldsymbol{\sigma}^2/2$ and $C[\boldsymbol{\sigma}] = \text{diag}(\boldsymbol{\sigma})$. The dynamic equation:*

$$(27) \quad \begin{aligned} \partial_t \boldsymbol{\sigma}(t) &= \frac{1}{2} \left(C[\boldsymbol{\sigma}(t)] |\nabla \mathbf{U} [\boldsymbol{\sigma}^2/2]|^2 - \boldsymbol{\sigma}(t) \right) = -\nabla_{\boldsymbol{\sigma}} \tilde{\mathcal{L}}(\boldsymbol{\sigma}(t)) , \\ \boldsymbol{\sigma}(0) &= \hat{\boldsymbol{\sigma}} > 0 , \end{aligned}$$

is the Gradient Flow in \mathbb{R}^m of the functional $\tilde{\mathcal{L}} = \mathcal{L} \circ \Psi$ given by:

$$(28) \quad \tilde{\mathcal{L}}(\boldsymbol{\sigma}) := \sup_{\mathbf{u} \in \mathbb{R}^n} \left\{ \mathbf{f}^T \mathbf{u} - \frac{1}{2} \mathbf{u}^T S \left[\frac{\boldsymbol{\sigma}^2}{2} \right] \mathbf{u} \right\} + \frac{1}{2} \mathbf{w}^T \frac{\boldsymbol{\sigma}^2}{2} .$$

Proof. The proof is a simple computation starting from Equation (20) replacing $\boldsymbol{\mu}$ with $\boldsymbol{\sigma}^2/2$. \square

Denoting with $\mathbf{z} = (\mathbf{u}, \boldsymbol{\sigma})$, the discretization of Equation (27) by backward Euler leads to the following sequence of non-linear systems of algebraic equations:

$$(29) \quad \mathbf{F}(\mathbf{z}) = \begin{pmatrix} \mathbf{F}_1(\mathbf{u}, \boldsymbol{\sigma}) \\ \mathbf{F}_2(\mathbf{u}, \boldsymbol{\sigma}) \end{pmatrix} = \begin{pmatrix} S[\boldsymbol{\sigma}^2/2] \mathbf{u} - \mathbf{f} \\ \boldsymbol{\sigma} - \boldsymbol{\sigma}^k - \Delta t_k \left(C[\boldsymbol{\sigma}] |\nabla \mathbf{u}|^2 - \boldsymbol{\sigma} \right) / 2 \end{pmatrix} = 0 .$$

The Jacobian matrix J can be calculated as:

$$(30) \quad J(\mathbf{u}, \boldsymbol{\sigma}) = \begin{pmatrix} S[\boldsymbol{\sigma}^2/2] & AC[\boldsymbol{\sigma}] G[\mathbf{u}] \\ -\Delta t_k C[\boldsymbol{\sigma}] G[\mathbf{u}] \nabla & D_3[\mathbf{u}] \end{pmatrix} ,$$

where D_3 is diagonal and given by:

$$D_3(\mathbf{u}) = \mathbf{1} - \frac{\Delta t_k}{2} \left(|\nabla \mathbf{u}|^2 - \mathbf{1} \right)$$

Inverting D_3 and substituting we obtain the final Newton linear system:

$$(31) \quad \begin{aligned} \tilde{M} \mathbf{s}_1 &= AC[\boldsymbol{\sigma}] G[\mathbf{u}] D_3[\mathbf{u}]^{-1} \mathbf{F}_2 - \mathbf{F}_1 \\ \mathbf{s}_2 &= D_3[\mathbf{u}]^{-1} \left(-\mathbf{F}_2 + \Delta t_k C[\boldsymbol{\sigma}] G[\mathbf{u}] \nabla \mathbf{s}_1 \right) , \end{aligned}$$

where \tilde{M} is given by:

$$\begin{aligned}\tilde{M} &= AC \left[\frac{\sigma^2}{2} \right] \nabla + \Delta t_k AC [\sigma^2] (G[\mathbf{u}])^2 \nabla \\ &= A \left(C \left[\frac{\sigma^2}{2} \right] + \Delta t_k C [\sigma^2] (G[\mathbf{u}])^2 D_3[\mathbf{u}]^{-1} \right) W^{-1} A^T,\end{aligned}$$

where again the square power for matrix G is intended element-by-element. As before, matrix $\tilde{M} = S[\tilde{\sigma}^2]$ can be written as the stiffness matrix S evaluated at $\tilde{\sigma}^2 = \{\tilde{\sigma}_e^2\}$, where:

$$(32) \quad \tilde{\sigma}_e^2 = \frac{\sigma_e^2}{2} + \Delta t_k \frac{\sigma_e^2 |\nabla \mathbf{u}_e|^2}{1 - \frac{\Delta t_k}{2} (|\nabla \mathbf{u}_e|^2 - 1)} = \frac{\sigma_e^2}{2} \frac{2 + \Delta t_k + 3\Delta t_k |\nabla \mathbf{u}_e|^2}{2 - \Delta t_k (|\nabla \mathbf{u}_e|^2 - 1)}$$

Note that system matrix \tilde{M} is Symmetric and Positive Definite (SPD) as long as Δt_k is small enough. In this case, the Jacobian matrix in Equation (30) can be written as a symmetric matrix simply by scaling the second block row by the factor $-(\Delta t_k)^{-1}W$. Our numerical implementation carries over directly from the implementation described in Section 4.1.

4.3. Numerical Experiments. We run the first benchmark case suggested in [19], which considers problem Equation (2) with unit weights ($\mathbf{w} = \mathbf{1}$). The $n \times m$ matrix A is dense and randomly generated with elements extracted from the standard normal distribution, normalized so that each row has unit Euclidean norm. The exact sparse solution \mathbf{q}^* is randomly generated with a random support of given dimension k and entries extracted from a uniform distribution in the interval $[-10, 10]$. The right-hand side is generated as $\mathbf{f} = A\mathbf{q}^*$. We build a sequence of four problems starting with $(n, m, k) = (250, 25000, 5) \times 2^{i-1}$, $i = 1, 2, 3, 4$. Note that the pre-imposed sparsity level k of the thought solution has no influence on the computational efficiency of our algorithm.

Simulation metrics include convergence towards steady state ($\text{var}(\boldsymbol{\mu}[t^k])$), relative error on the exact solution, and constraint error in the dual BP problem (see Equation (16)), the last two defined as:

$$\text{err}_{\mathbf{q}^*}(\mathbf{q}[t^k]) := \frac{\|\mathbf{q}[t^k] - \mathbf{q}^*\|}{\|\mathbf{q}^*\|} \quad \text{err}_{\text{Dual}}(\mathbf{u}[t^k]) = |(\|A^T \mathbf{u}[t^k]\|_\infty - 1)|.$$

All the runs are conducted on a 3.4GHz Intel-I7 (1-core) CPU.

Physarum Dynamics. Figure 1 reports the results for the four different problems. We first observe that the three metrics have a common time-evolution, differing only by a multiplicative constant in the log-log plots in the left column. Future studies will be devoted to analyze their relationship so that better error estimators can be used to develop more efficient time-step strategies. Secondly, we would like to emphasize the distance between time-steps that increases progressively as steady state is approach, a consequence of our empirical time-step adaptation strategy.

The column on the right, showing the behavior of the three metrics with respect to CPU time, shows that some time steps are less CPU efficient than others, as indicated by visibly smaller slopes of the interpolation lines between consecutive metric samples in particular towards the lower accuracy levels. To discuss this occurrence, we focus on the first problem set (top-right figure) and look at the 16-th time step ($t_{CPU} \in [19, 20]$ sec). The empirical time-stepping strategy initially over-estimated Δt_{16} and this forced a re-assembly of the dense matrix and its Choleski factorization for a number of times, thus drastically contributing to the loss of computing time. The development of problem-adapted preconditioning strategies such as those proposed by [11, 5] will be considered in the future for better performance.

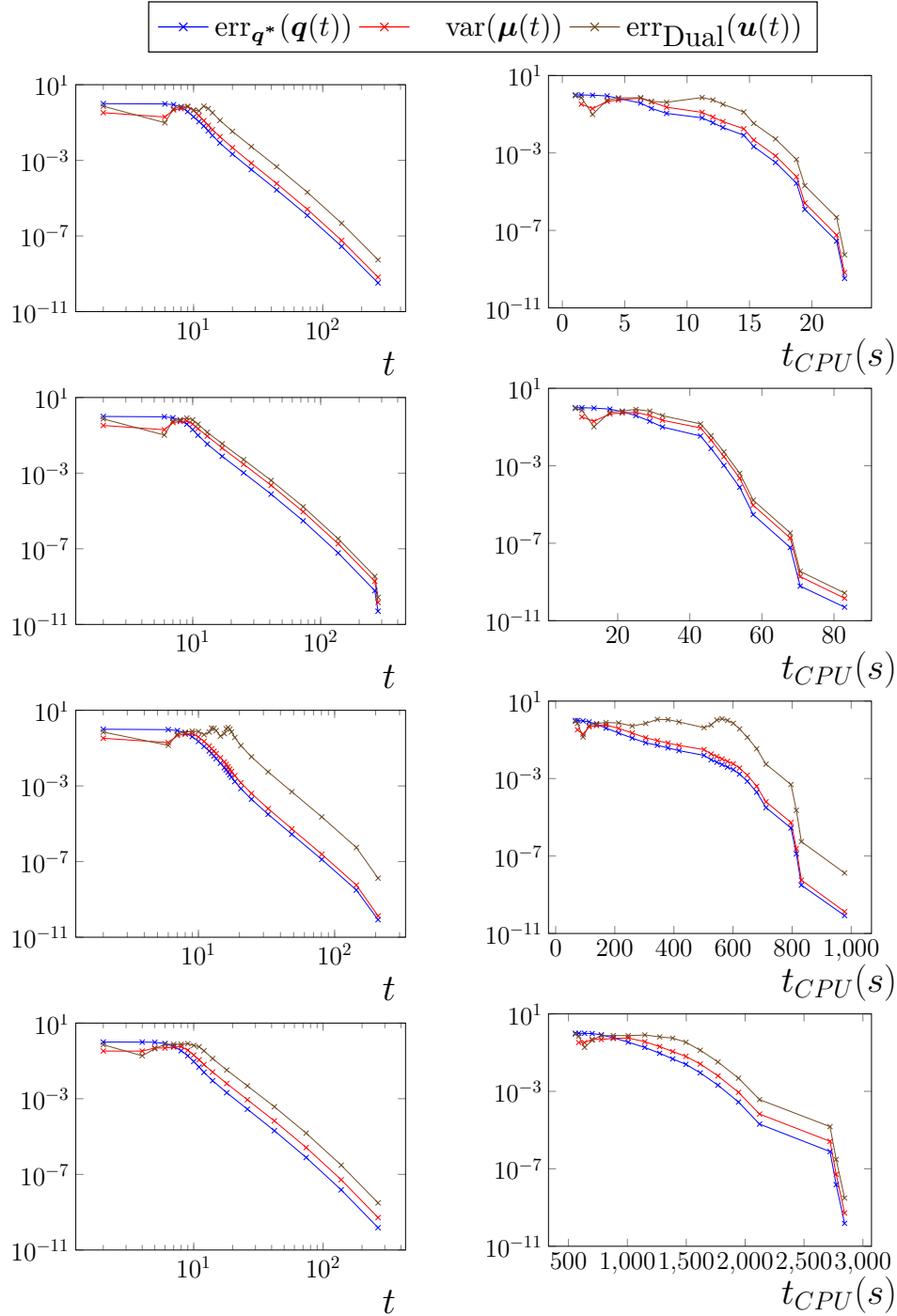


FIGURE 1. Numerical results for PD . Left column: time (t) evolution of $\text{var}(\boldsymbol{\mu}[t])$, $\text{err}_{q^*}(\mathbf{q}[t])$, and $\text{err}_{\text{Dual}}(\mathbf{u}[t])$ for the four test problems. The values are sampled at every time-step t^k (indicated with crosses) and completed by linear interpolation. Right column: values of the three simulation metrics as a function of computational time (seconds of CPU).

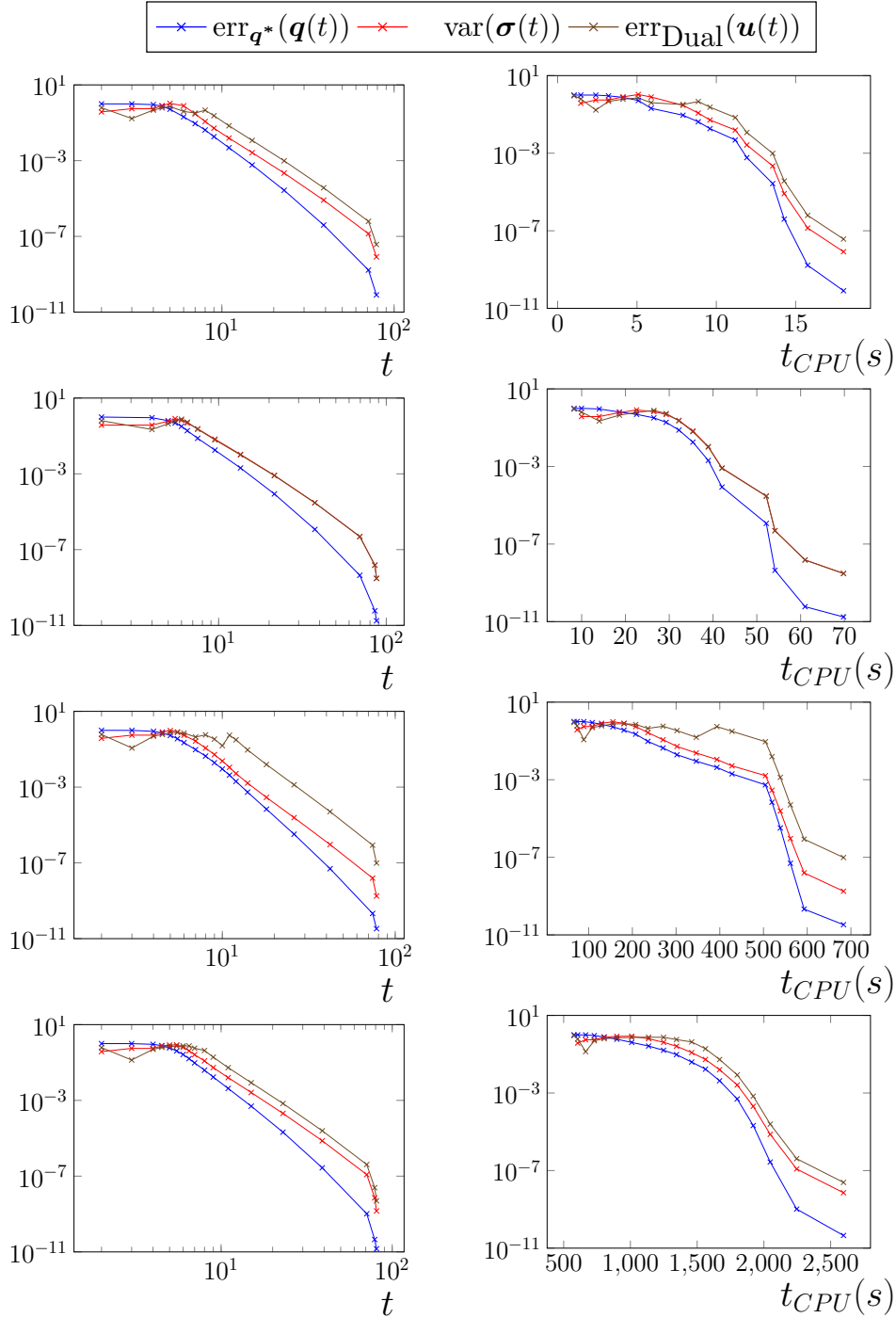


FIGURE 2. Numerical results for GF. Left column: time (t) evolution of $\text{var}(\boldsymbol{\sigma}[t])$, $\text{err}_{q^*}(\mathbf{q}[t])$, and $\text{err}_{\text{Dual}}(\mathbf{u}[t])$ for the four test problems. The values are sampled at every time-step t^k (indicated with crosses) and completed by linear interpolation. Right column: values of the three simulation metrics as a function of computational time (seconds of CPU).

Gradient Flow for Basis Pursuit. Figure 2 reports the numerical results on the same sets of test problems using the gradient flow approach. The convergence profiles are similar to the PD case, with the only exception that $\text{err}_{q^*}(\mathbf{q}[t])$ is characterized by a higher asymptotic slope than $\text{var}(\boldsymbol{\sigma}[t])$ and $\text{err}_{\text{Dual}}(\mathbf{u}[t])$. Moreover, the slightly different time-step size sequence causes different numbers and localizations of the back-stepping and matrix re-assembly phases. The overall performance is globally the same.

5. CONCLUSIONS

We have presented an efficient numerical implementation of the Physarum dynamics algorithm using a dynamic Monge-Kantorovich perspective for the solution of general basis pursuit problems. We show existence and uniqueness of the solution for all times and introduce a Lyapunov functional with decreasing derivative along the trajectories. We show that a simple modification of the proposed approach leads to a gradient flow for the Lyapunov functional. This provides a reinterpretation of the Physarum dynamics as a gradient descent method offering a renewed perspective to enhance computational efficiency of these class of algorithms.

Our current implementation, based on combining implicit time-stepping with Inexact Newton-Krylov methods, is shown to be accurate, robust and efficient in solving basis pursuit benchmark problems taken from the literature.

ACKNOWLEDGMENTS

This work was partially funded by the the UniPD-SID-2016 project Approximation and discretization of PDEs on Manifolds for Environmental Modeling and by the EU-H2020 project ‘‘GEOEssential-Essential Variables workflows for resource efficiency and environmental management’’, project of ‘‘The European Network for Observing our Changing Planet (ERA-PLANET)’’, GA 689443.

REFERENCES

- [1] A. BECK, *On the convergence of alternating minimization for convex programming with applications to iteratively reweighted least squares and decomposition schemes*, SIAM J. Sci. Opt., 25 (2015), pp. 185–209.
- [2] L. BERGAMASCHI, E. FACCA, A. MARTÍNEZ CALOMARDO, AND M. PUTTI, *Spectral preconditioners for the efficient numerical solution of a continuous branched transport model*, J. Comput. Appl. Math., Submitted (2017).
- [3] V. BONIFACI, K. MEHLHORN, AND G. VARMA, *Physarum can compute shortest paths*, J. Theor. Biol., 309 (2012), pp. 121–133.
- [4] G. BOUCHITTÉ, G. BUTTAZZO, AND P. SEPPECHER, *Shape optimization solutions via Monge-Kantorovich equation*, C. R. Math. Acad. Sci. Paris, 324 (1997), pp. 1185–1191.
- [5] I. DASSIOS, K. FOUNTOULAKIS, AND J. GONDZIO, *A preconditioner for a primal-dual Newton conjugate gradient method for compressed sensing problems*, SIAM J. Sci. Comput., 37 (2015), pp. A2783–A2812.
- [6] R. S. DEMBO, S. C. EISENSTAT, AND T. STEIHAUG, *Inexact Newton methods*, SIAM J. Num. Anal., 19 (1982), pp. 400–408.
- [7] I. EKELAND AND R. TÉMAM, *Convex Analysis and Variational Problems*, Classics in Applied Mathematics, Society for Industrial and Applied Mathematics, 1999.
- [8] L. C. EVANS AND W. GANGBO, *Differential equations methods for the Monge–Kantorovich mass transfer problem*, vol. 653, American Mathematical Soc., 1999.
- [9] E. FACCA, F. CARDIN, AND M. PUTTI, *Towards a stationary Monge–Kantorovich dynamics: The Physarum Polycephalum experience*, SIAM J. Appl. Math., 78 (2018), pp. 651–676.
- [10] E. FACCA, S. DANERI, F. CARDIN, AND M. PUTTI, *Numerical solution of Monge-Kantorovich equations via a dynamic formulation*, SIAM J. Sci. Comput., Submitted (2018).
- [11] K. FOUNTOULAKIS, J. GONDZIO, AND P. ZHLOBICH, *Matrix-free interior point method for compressed sensing problems*, Math. Prog., 6 (2013), pp. 1–31.
- [12] P. HARTMAN, *Ordinary Differential Equations: Second Edition*, Classics in Applied Mathematics, Society for Industrial and Applied Mathematics, 2001.

- [13] C. T. KELLEY, *Numerical methods for nonlinear equations*, Acta Num., 27 (2018), pp. 207–287.
- [14] T. NAKAGAKI, H. YAMADA, AND A. TOTH, *Maze-solving by an amoeboid organism*, Nature, 407 (2000), pp. 470–470.
- [15] D. STRASZAK AND N. K. VISHNOI, *IRLS and slime mold: Equivalence and convergence*, ArXiv e-prints, (2016).
- [16] A. TERO, R. KOBAYASHI, AND T. NAKAGAKI, *A mathematical model for adaptive transport network in path finding by true slime mold*, J. Theor. Biol., 244 (2007), pp. 553–564.
- [17] A. TERO, S. TAKAGI, T. SAIGUSA, K. ITO, D. P. BEBBER, M. D. FRICKER, K. YUMIKI, R. KOBAYASHI, AND T. NAKAGAKI, *Rules for biologically inspired adaptive network design*, Science, 327 (2010), pp. 439–442.
- [18] C. VILLANI, *Optimal Transport*, vol. 338 of Old and New, Springer Science & Business Media, Berlin, Heidelberg, 2008.
- [19] A. Y. YANG, S. S. SASTRY, A. GANESH, AND Y. MA, *Fast l_1 -minimization algorithms and an application in robust face recognition: A review*, in Image Processing (ICIP), 2010 17th IEEE International Conference on, IEEE, 2010, pp. 1849–1852.

DEPARTMENT OF MATHEMATICS, UNIVERSITY OF PADUA, VIA TRIESTE 63, PADOVA, ITALY,
{FACCA,CARDIN,PUTTI}@MATH.UNIPD.IT